

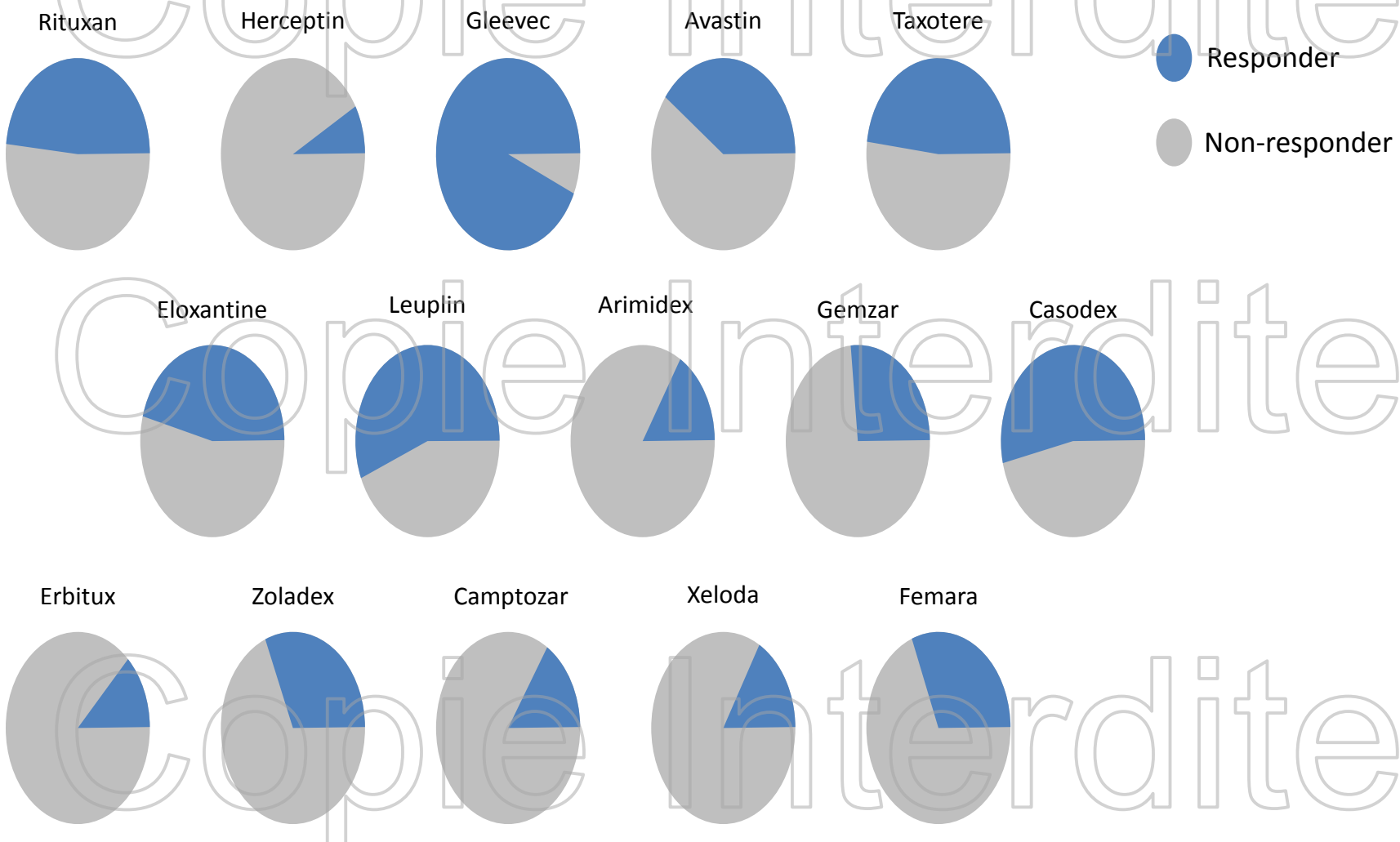
ONCOLOGIE NUCLEAIRE THERANOSTIQUE

F. COURBON , M BAURIAUD, C FONTAN , E. GABIACHE, S BRILLOUET



**INSTITUT UNIVERSITAIRE
DU CANCER DE TOULOUSE
Oncopole**

La cancérologie et ses échecs



Jackson DB, Clinical and economic impact of the non-responder problem;
Drug Discovery Today, April 2009; Analysis of FDA label data for top 15 drugs

THERANOSTIC

LE CONCEPT :

CIBLE + → TRAITEMENT +
CIBLE - → TRAITEMENT -

Rôle de l'imagerie

Taxonomie :

expression de cible,
pronostic cTNM > vascularisation > nécrose > signal biologique

Réponse

Critère de substitution/ précoce d'efficacité

PK

Phase R0

Vous avez dit : « Théranostique »

On en fait depuis longtemps

tout ce qui n'est pas prose est vers et tout ce qui n'est point vers est prose !



RADIOOTHERAPIE INTERNE VECTORISEE

NIS :131I Kc de la thyroïde

NA :131ImIBG Neuroblastomes, T endocrines

CD20 : 90Y-MoAb LMNH

SSTr :177Lu ou 90Y ou 111In -peptide T endocrines

Annals of Oncology Advance Access published April 13, 2007

review

Annals of Oncology
doi:10.1093/annonc/mdm111

Targeted therapy in nuclear medicine—current status and future prospects

W. J. G. Oyen^{1,2*}, L. Bedel^{1,3}, F. Giannarini^{1,4}, H. R. Maecke^{1,5}, J. Tennvall^{1,6},
M. Luster^{1,7} & B. Brans^{1,8}

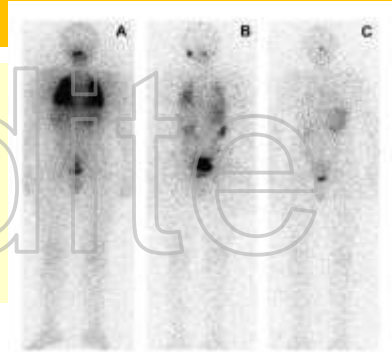
TEP¹⁸FDG...

CIBLE + → TRAITEMENT +

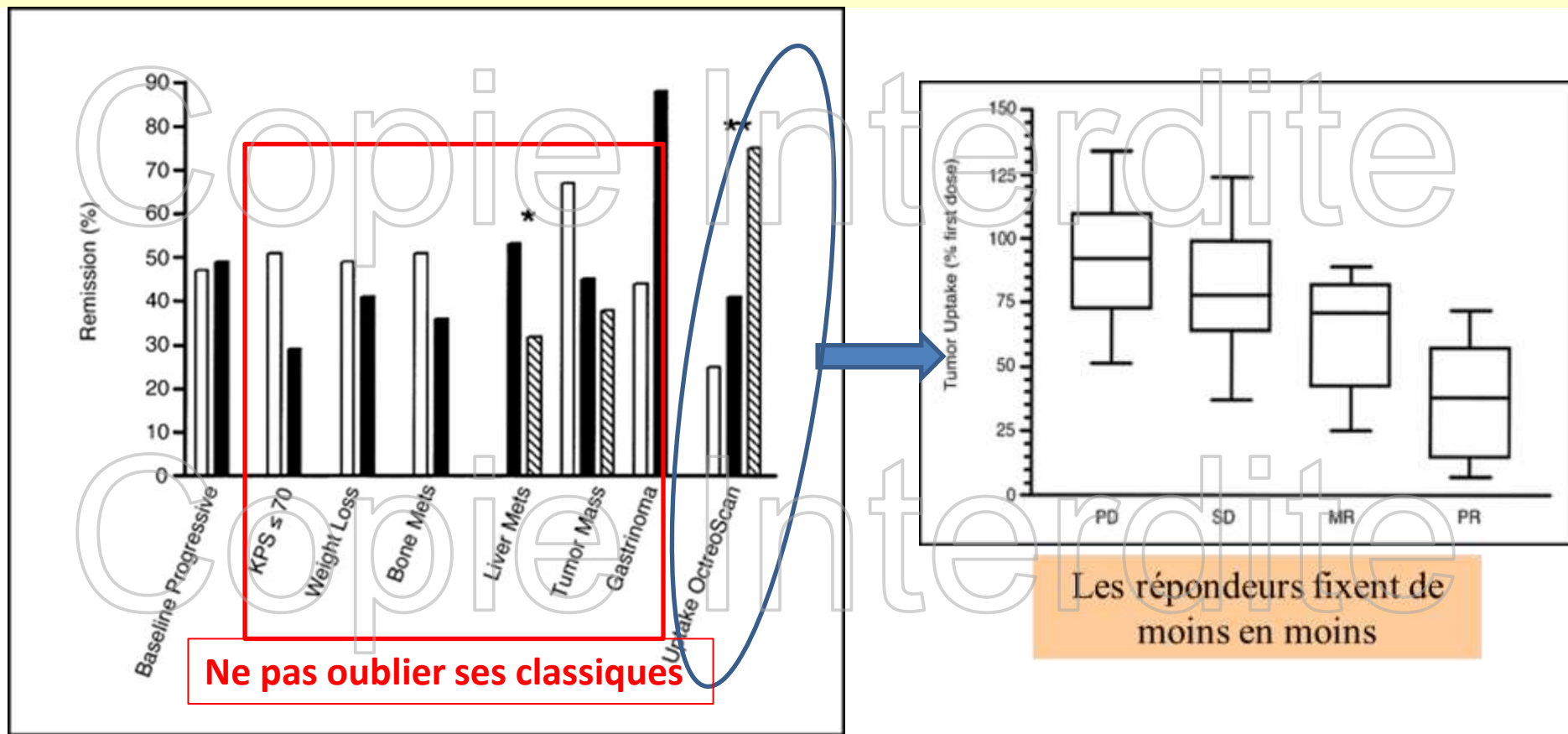
131-I et Cancer de la thyroïde

En général I131 + → REPONSE +

Oyen et al 2007

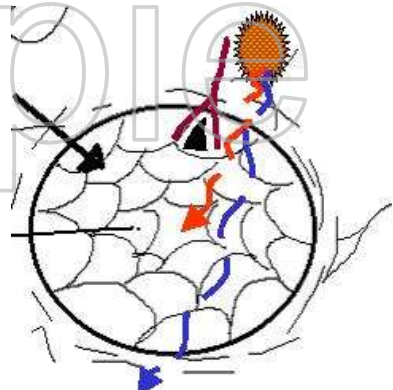


90Y, 177 Lu – SMS analogues T Endocrines



CIBLE + → TRAITEMENT + SOUS CONDITION

1° La taille



Zevalin (0.4mCi/Kg) vs Rituximab Witzig et al JCO 2002

ORR 80% vs 56 %

CR 30% vs 16%

TPP 17.8 m vs 11.2 LF

2° le nombre de cibles

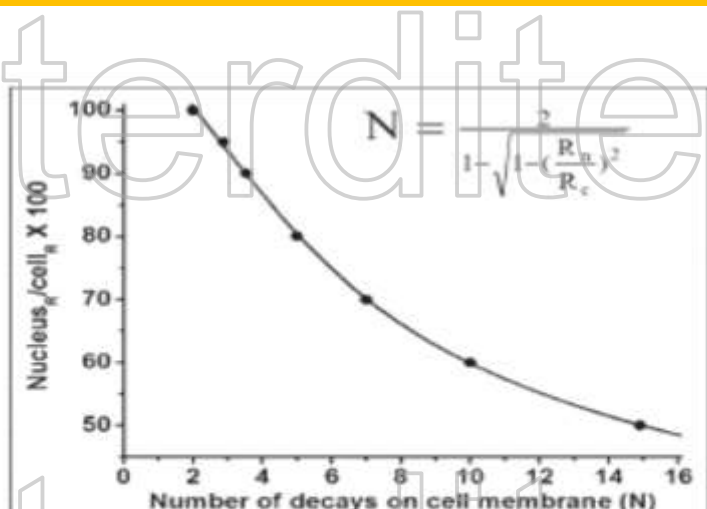


FIGURE 1. Number of radioactive atoms needed to assure traversal of cell nucleus by a single energetic particle as function of distance from nuclear membrane. Nuclear-to-cell radius (percentage) plotted as function of number of decays in cell membrane.

Pas d'antigène spécifique d'une prolifération tumorale

Par défaut:

100 fois plus par les cellules tumorales,

> 500000 sites par cellules,

constante d'affinité > 10^8 M^{-1}

CIBLE + → TRAITEMENT + : Pas systématique

Caractérisation fonctionnelle et Réponse tumorale $16\alpha-[18\text{F}]$ fluoro-17-estradiol

Kc du sein

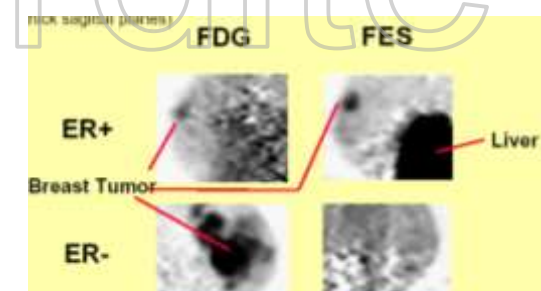
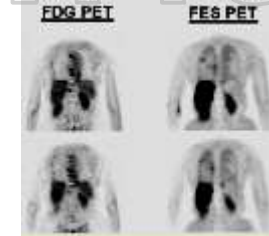
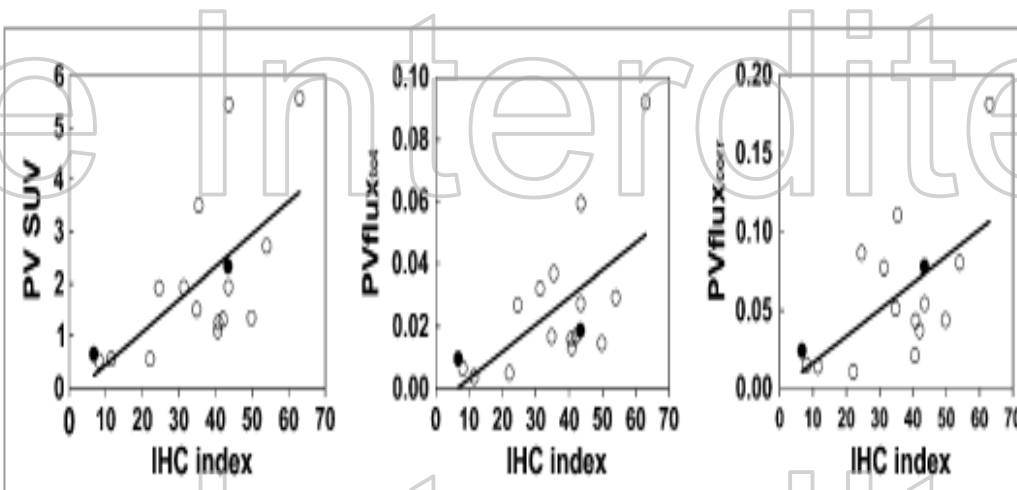


FIGURE 5. Comparison of ^{18}F -FES uptake measures with IHC index (Photoshop analysis). Treated patients are identified by closed circles.



Quantitative Imaging of Estrogen Receptor Expression in Breast Cancer with PET and ^{18}F -Fluoroestradiol

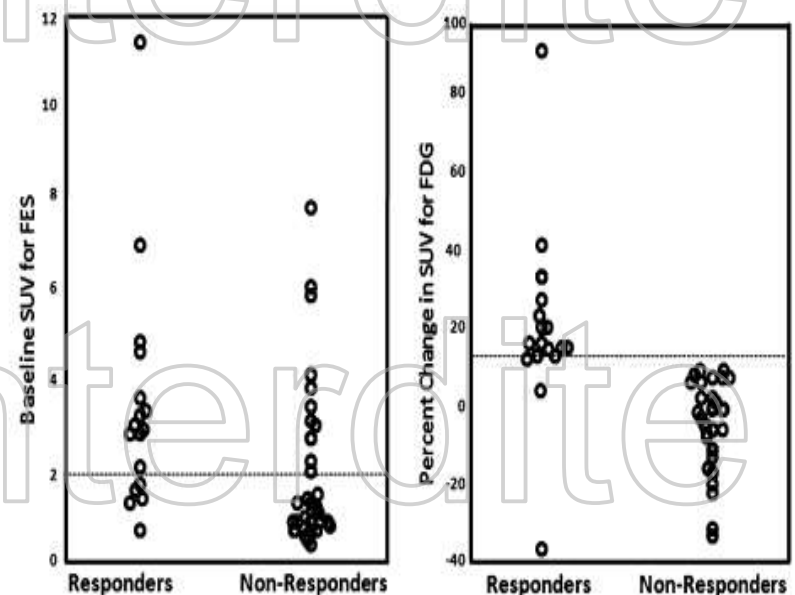
Différence entre voir une cible et tester une cible :



FGD FES

Fig. 2 The baseline tumor FES (left) and percent change in tumor FDG (right) uptake after estradiol challenge in patients who responded and who did not respond to endocrine therapy

Test de stimulation par
œstrogènes



Breast Cancer Res Treat (2009) 113:509–517
DOI 10.1007/s10549-008-9953-0

CLINICAL TRIAL

PET-based estradiol challenge as a predictive biomarker
of response to endocrine therapy in women
with estrogen-receptor-positive breast cancer

FDG Flair up

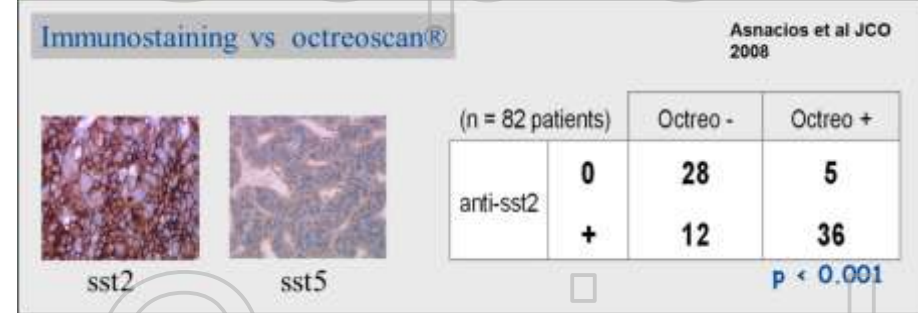
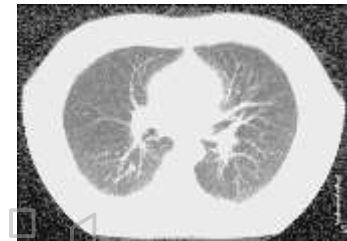
•CIBLE – ➔ PAS DE CIBLE

Outcome of Differentiated Thyroid Cancer with Detectable Serum Tg and Negative Diagnostic ^{131}I Whole Body Scan: Comparison of Patients Treated with High ^{131}I Activities Versus Untreated Patients

2001

Treatment of iodine-negative thyroglobulin-positive thyroid cancer: differences in outcome in patients with macrometastases and patients with micrometastases

EJNM 20004



68Ga-DOTA-Tyr3-Octreotide PET in Neuroendocrine Tumors: Comparison with Somatostatin Receptor Scintigraphy and CT Virgolini et al JNM 2007

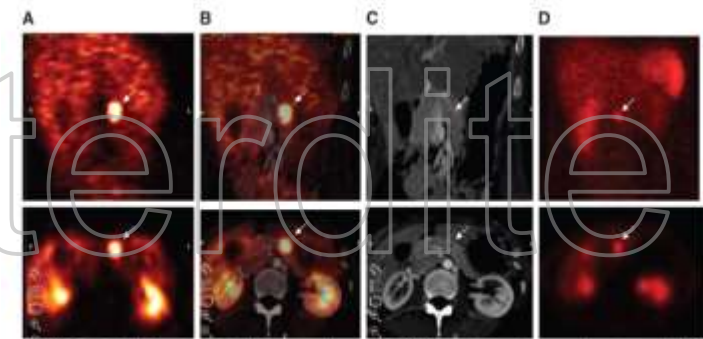


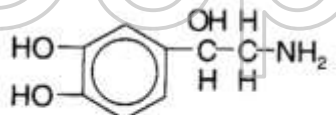
FIGURE 1. A 28-y-old female was referred for primary diagnosis of a NET because of elevated tumor markers in serum. PET (A) clearly depicted an abnormal focus in upper abdomen (arrow). This lesion could be delineated in the pancreas after image fusion with CT (B). There was also increased contrast medium enhancement in the margin when using helical CT/ICL SPECT with ^{68}Ga -HYNIC-TOD (C) was also positive for this tumor in upper abdomen (D). This positive finding was confirmed by histopathology revealing a NET with 1 cm in diameter. (Top) Coronal views; (bottom) axial views.

68Ga-DOTA-Tyr3-Octreotide PET > CT

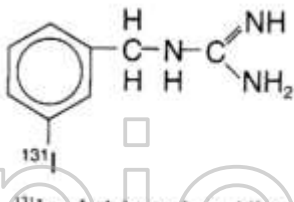
68Ga-DOTA-Tyr3-Octreotide PET > SRS

• CIBLE – ➔ PAS DE CIBLE

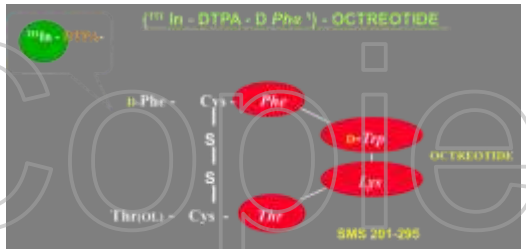
Interférences médicamenteuses



Noradrenaline



^{131}I -m-Iodobenzylguanidine



Analogue froids de la SMS

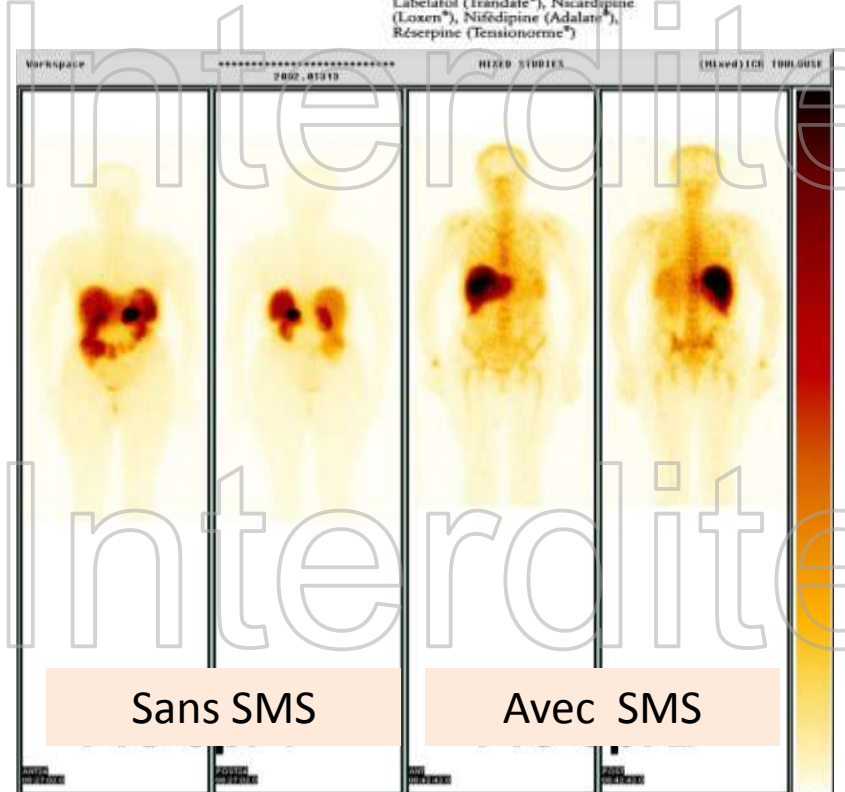
Interférences médicamenteuses (liste non exhaustive).

Antidépresseurs :

- médicaments qui contiennent Amtriptyline (Elavil®), Loxapac®, Amitriptyline (Defanyl®), Clomipramine (Anafranil®), Désipramine (Pertofract®), Dosulépine (Prothiadén®), Dexépine (Sinequan®), Maprotiline (Ludionil®), Opiprétamol (Insadon®), Quinupramine (Kunupri®), Trimipramine (Surmontil®).

Antihypertenseurs, bêta-bloquants ou autres :

- médicaments qui contiennent Cordarone[®], Digitoxine (Digitaline[®]), Digoxine[®], Israpidine (Icaz[®]), Labelatul (Trandate[®]), Nicardipine (Loxen[®]), Nifédipine (Adalat[®]), Réserpine (Tensionorme[®])



CIBLE -



PAS DE TRAITEMENT -

SRS pas de Valeur prédictive de l'efficacité de thérapeutique

Vezzosi et al European Journal of Endocrinology, 2005

Mieux vaut faire un test thérapeutique



Clinical Endocrinology (2008) 68, 904–911

doi:10.1111/j.1365-2265.2007.03136.x

ORIGINAL ARTICLE

Short- and long-term somatostatin analogue treatment in patients with hypoglycaemia related to endogenous hyperinsulinism

D. Vezzosi*, A. Bennet*, F. Courbont and P. Caron*

*Department of Endocrinology and †Department of Nuclear Medicine, Centre Hospitalier Universitaire, Toulouse, France

Cible fonctionnelle → imagerie Fonctionnelle : Restauration de fonction

Ex perméabilité péritonéale / Carcinose P

Comparison of peritoneal equilibration test with ^{99m}Tc -DTPA excretion in the assessment of peritoneal permeability

B. K. Das¹, M. S. Senthilnathan¹, P. K. Pradhan¹, S. Nagabhushan¹, T. K. Jeloka², R. K. Sharma²

¹ Department of Nuclear Medicine, Sanjay Gandhi Postgraduate Institute of Medical Sciences, Lucknow, India

² Department of Nephrology, Sanjay Gandhi Postgraduate Institute of Medical Sciences, Lucknow, India

Received: 28 August 2003 / Accepted: 31 December 2003 / Published online: 18 February 2004

© Springer-Verlag 2004

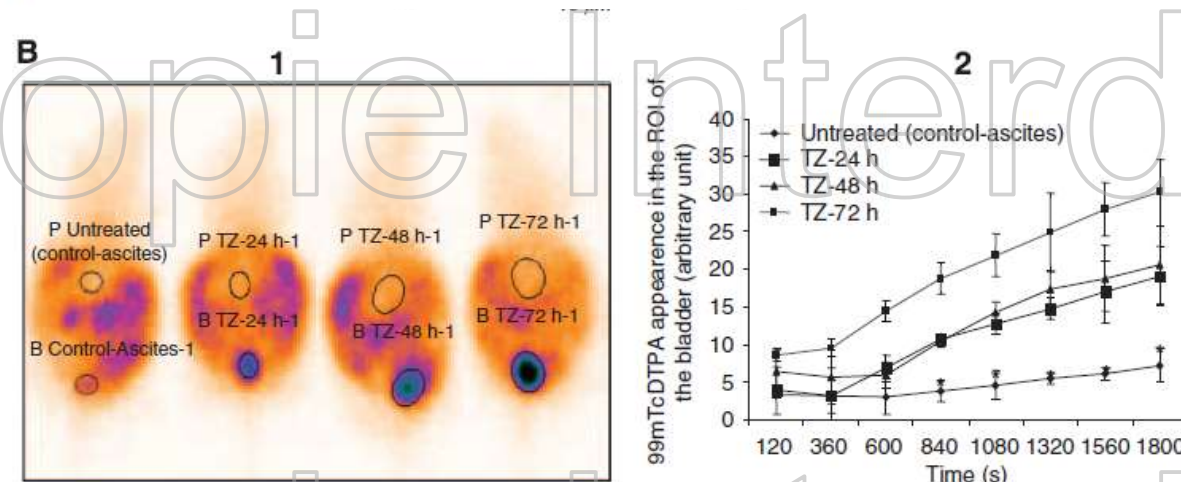


Figure 1 (A) Pathological pattern of the peritoneum 20 days after OVCAR-3 WT implantation. Nude mice bearing OVCAR-3 macroscopic ascites were treated with vehicle (A1) or trastuzumab at a dose of 150 $\mu\text{g}/\text{ml}$ per day (A2) administered by i.p. route for 72 h. Naive nude mice were i.p. injected once a day for 3 days with 1 ml of either RPMI-1640 (A3 control group) or the 24 h serum-free cleared supernatant collected from OVCAR-3 cells in culture (A4). Mice were killed and the peritonea were collected and formalin fixed. Microscopic examination was performed and pictures were taken. (B) Concentrations of ^{99m}Tc -DTPA over time in the bladder: peritoneal permeability. ^{99m}Tc -DTPA appeared in the bladder more intensively in treated animals compared with the untreated group. Arbitrary units express the ^{99m}Tc -DTPA intensity detection in the region of interest (ROI) of the bladder (shortened by 'B' and by 'P' for the peritoneum). * $P < 0.05$. Student's t-test compared untreated group (control-ascites) with trastuzumab (TZ) treatment groups.

innovations thérapeutiques

Copie Interdite

Théranostique : quelle méthode choisir ?

- Identifier une cible
- Evaluer précocement une altération métabolique

**Clinical Cancer
Research**

Nuclear Imaging Probes: from Bench to Bedside

Hans-Jürgen Wester

Clin Cancer Res 2007;13:3470-3481. Published online June 15, 2007.



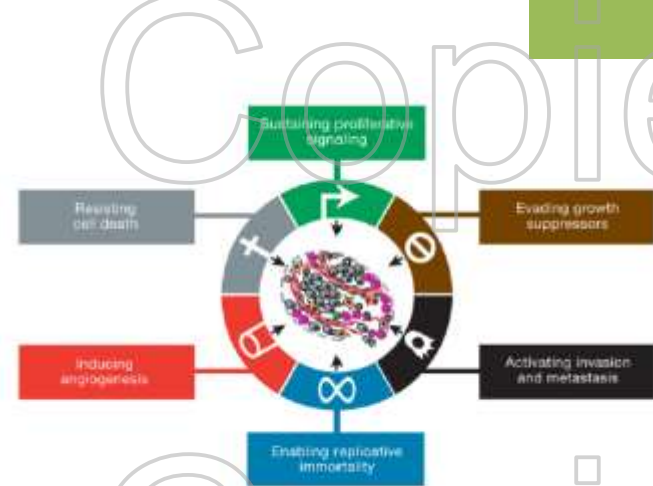
Tumor Cell Metabolism Imaging

JNM 2008

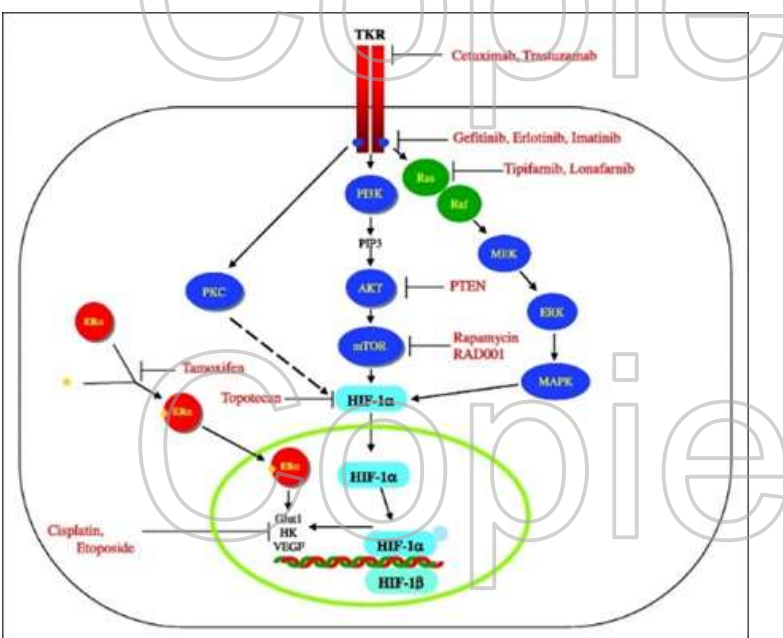
Christian Pfleiderer^{1,2} and Wolfgang A. Weber¹

¹Department of Nuclear Medicine, University of Freiburg, Freiburg, Germany; and ²Department of Radiology, German Cancer Research Center, Heidelberg, Germany

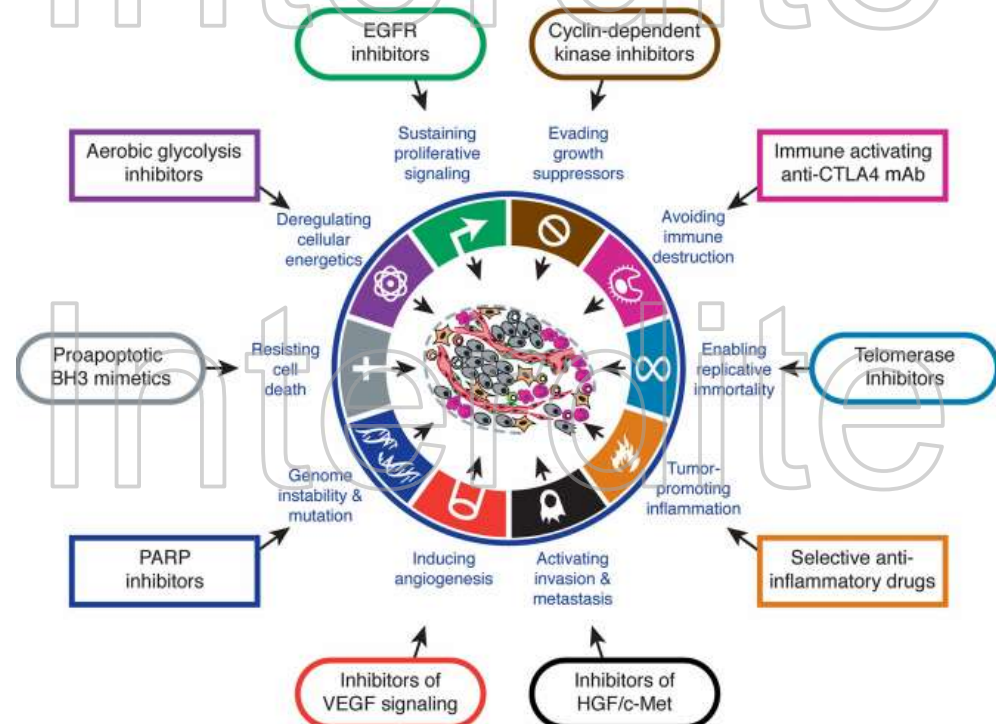
Métabolisme



Années 2000



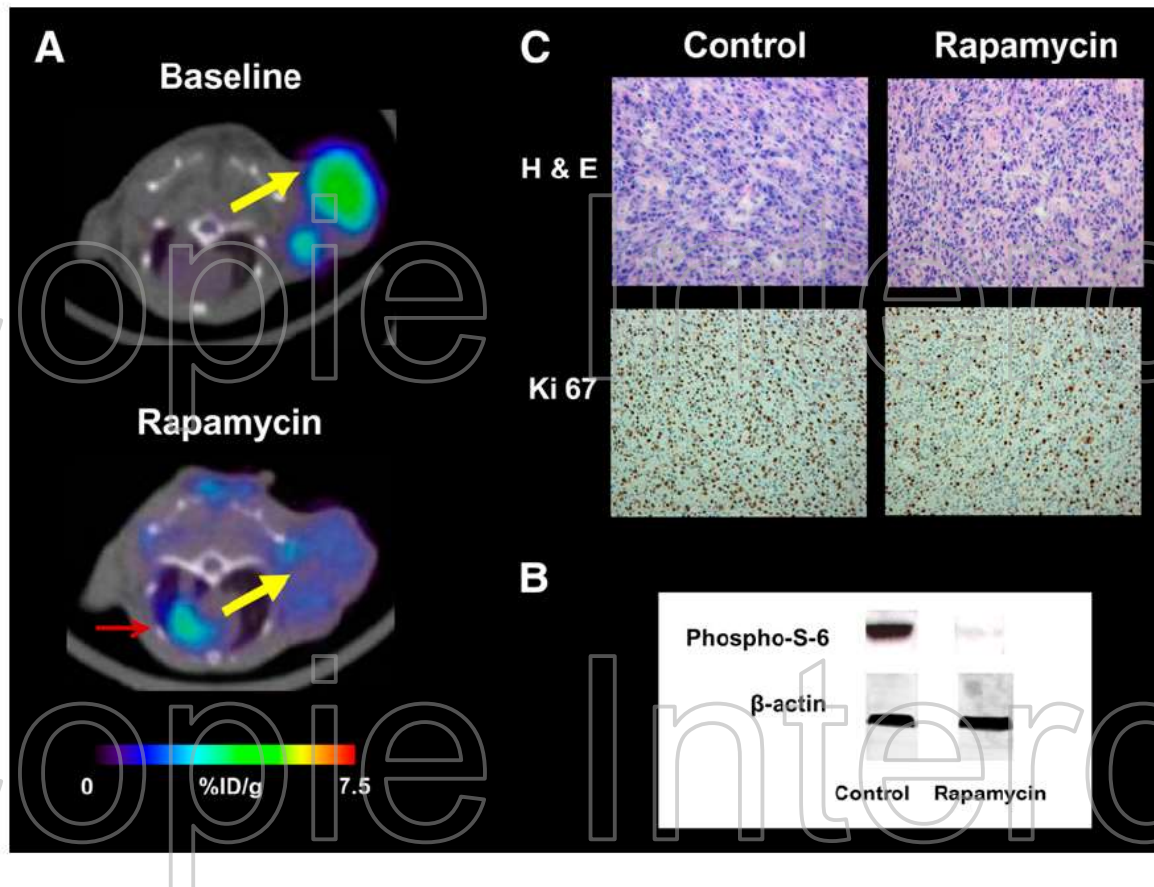
D Sullivan. Clinical Cancer Research Vol. 11, 2785-2808,
April 15, 2005



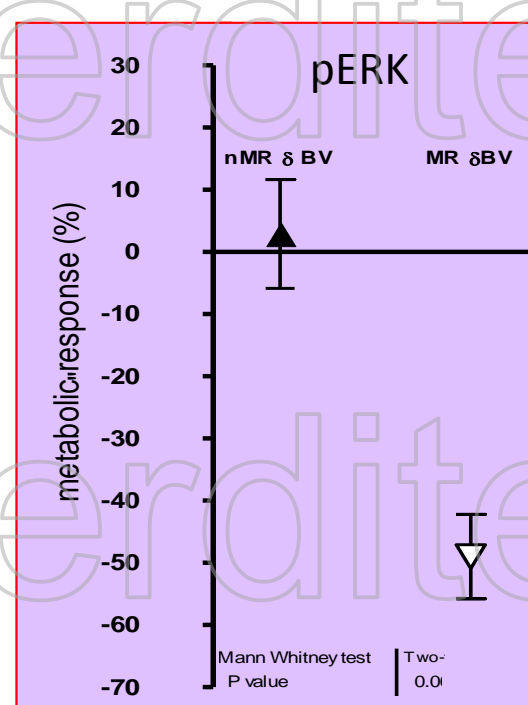
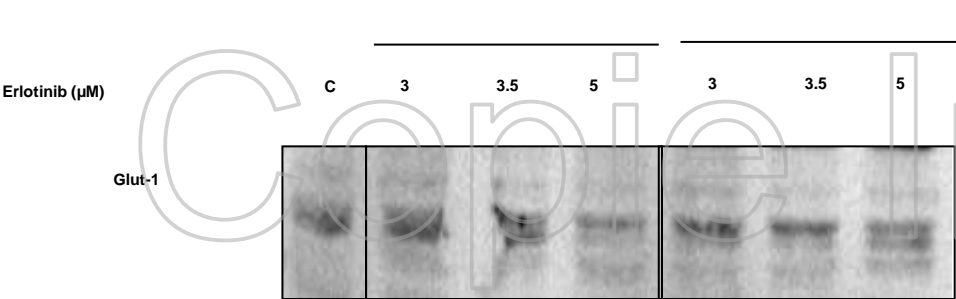
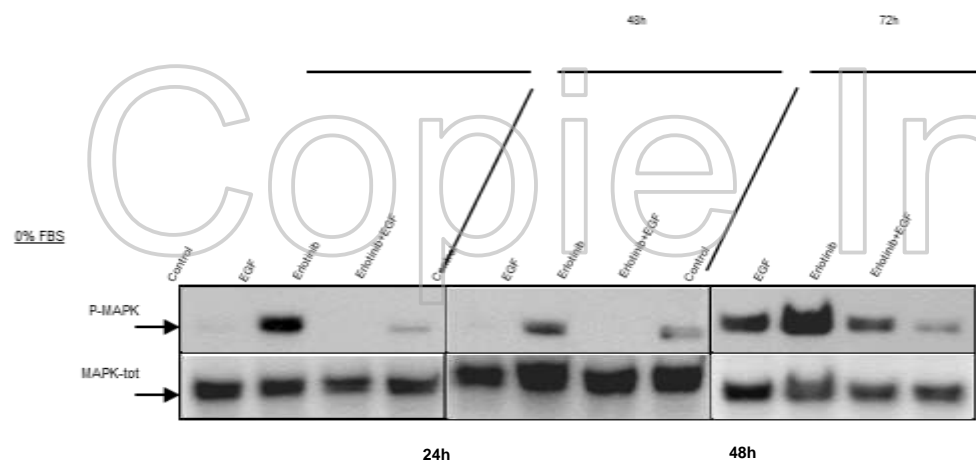
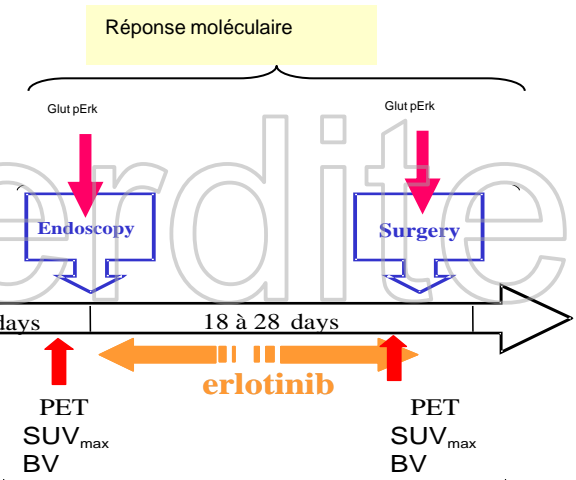
Hanahan D, Cell, 2011; 144:646-74

FDG un traceur spécifique !

mTORi et TEP FGD



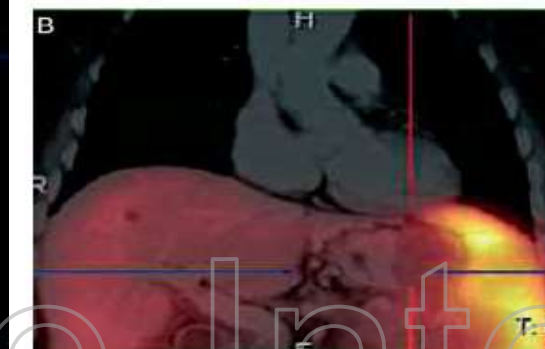
Tk_i Confirmation des souris aux humains



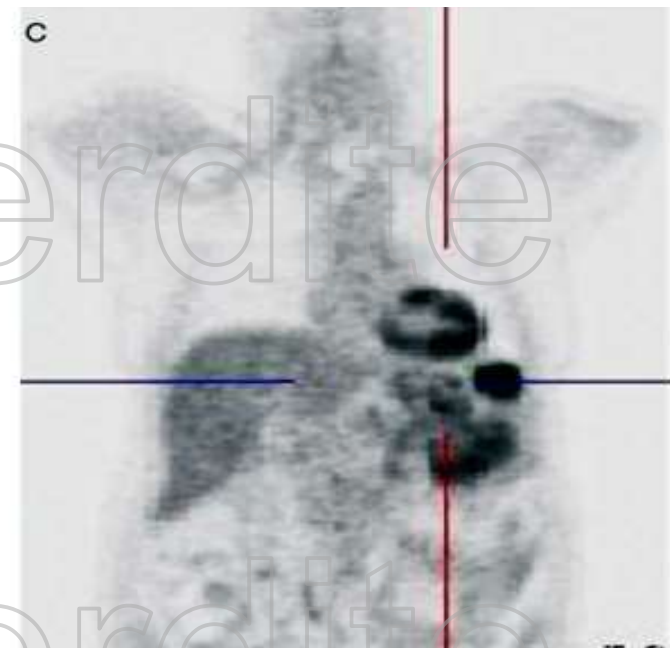
Vergez et al Clin Can Res 2007 -2010

^{18}FDG TEP : le paraddigme

- 1. Pronostic (ex Garin et al. pour les TE)**
- 2. Evaluation de la réponse**



SST neg



FDG pos.

Théranostic et MoAb marqués

Eur J Nucl Med Mol Imaging (2012) 39:512–520
DOI 10.1007/s00259-011-2008-5

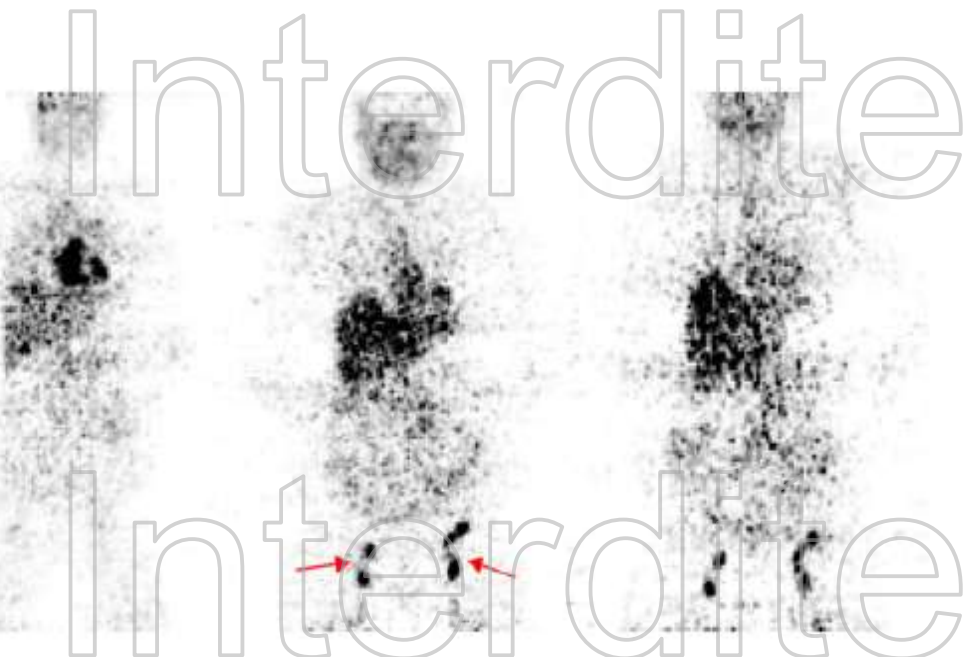
ORIGINAL ARTICLE

Biodistribution, radiation dosimetry and scouting of ^{90}Y -ibritumomab tiuxetan therapy in patients with relapsed B-cell non-Hodgkin's lymphoma using ^{89}Zr -ibritumomab tiuxetan and PET

Saiyada N. F. Rizvi · Otto J. Visser ·

Fig. 1 Typical coronal section ^{89}Zr -ibritumomab tiuxetan images at 1, 72 and 144 h p.i.
Arrows indicate tumour localizations

The dose-limiting organ in patients undergoing stem cell transplantation is the liver.



Le foie vous dis-je!



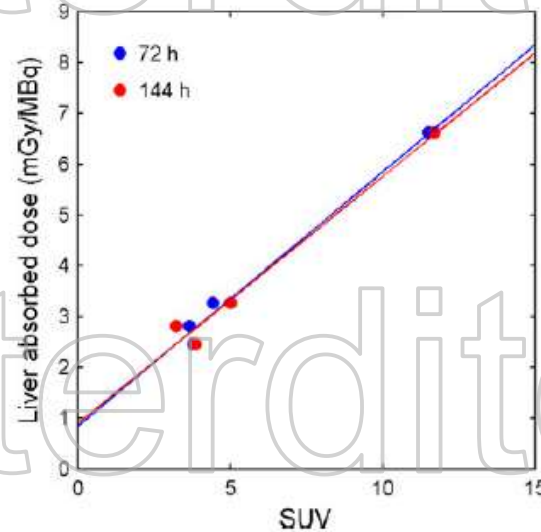
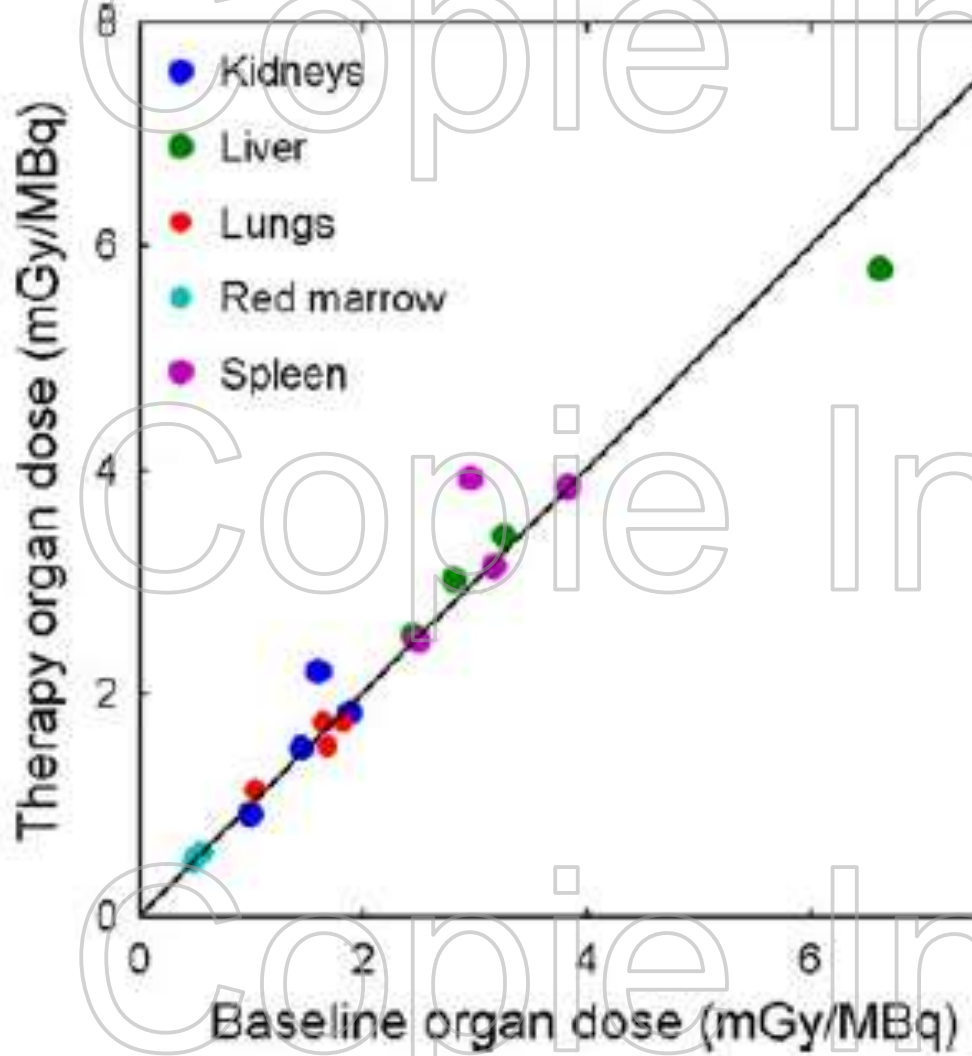


Fig. 5 Absorbed ^{90}Y dose to the liver, based on scout scans with ^{89}Zr -ibritumomab tiuxetan, versus SUV of ^{89}Zr -ibritumomab tiuxetan at 72 and 144 h p.i. The solid lines represent linear fits to the data

Apres le SUV ... la texture :

Mais que diable allait-il faire dans cette galère?



Hanaoka et al. EJNMMI Research (2015) 5:10
DOI 10.1186/s13550-015-0093-3

EJNMMI Research
a SpringerOpen Journal

ORIGINAL RESEARCH

Open Access

Heterogeneity of intratumoral ^{111}In -ibritumomab tiuxetan and ^{18}F -FDG distribution in association with therapeutic response in radioimmunotherapy for B-cell non-Hodgkin's lymphoma

Kohei Hanaoka¹, Makoto Hosono^{2*}, Yoichi Tatsumi³, Kazunari Ishii⁴, Sung-Woon Im¹, Norio Tsuchiya², Kenta Sakaguchi² and Itaru Matsumura³

Du SUV à la texture, Vicini et al 1997, Baek et al 2012 !

quantification of the spatial heterogeneity of voxel-based activities

$$\text{Skewness} = \frac{1}{n} \sum_{i=1}^n (x_i - \bar{x})^3 / s^3$$

$$\text{Kurtosis} = \frac{1}{n} \sum_{i=1}^n (x_i - \bar{x})^4 / s^4$$

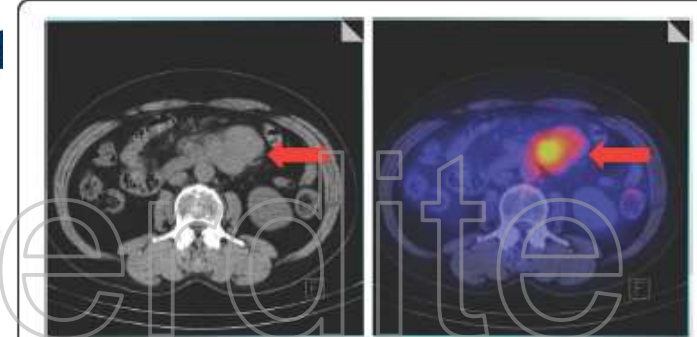


Figure 4 Representative CT and fused image of the markedly accumulation of ^{111}In -ibritumomab tiuxetan in the para-aortic lymph node (arrow). A male patient with B-cell non-Hodgkin's lymphoma had a standardized uptake value of para-aortic lymph node of 3.81, skewness of 0.813, kurtosis of 2.95, and AUC-CSH of 0.344.

PREDICTION FDG > RX

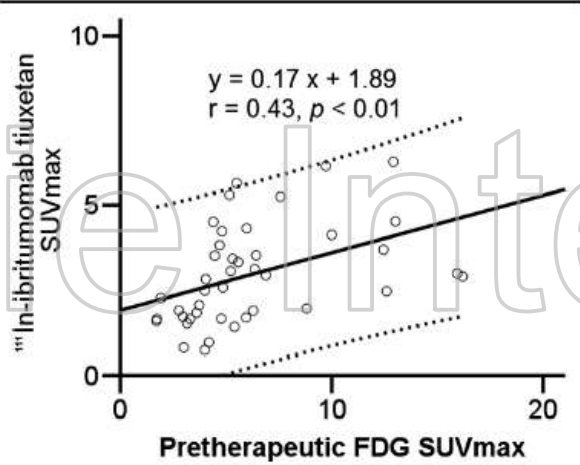


Figure 2 Correlation between pretherapeutic FDG SUVmax and ¹¹¹In-ibritumomab tiuxetan SUVmax in all lesions. The solid line is the progression line. Dotted lines represent 95% confidence intervals of the progression line.

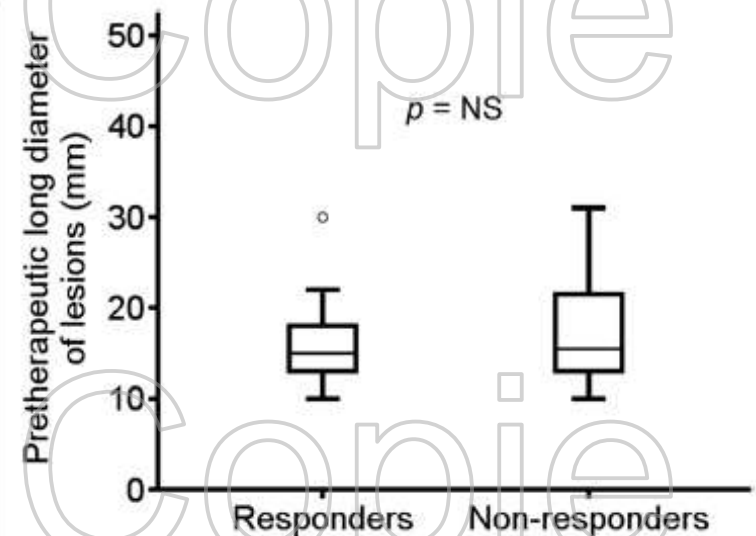


Figure 1 Comparison of the diameter (mm) of pretherapeutic lesions between responders and non-responders. The median value and the interquartile range are represented by box plot.

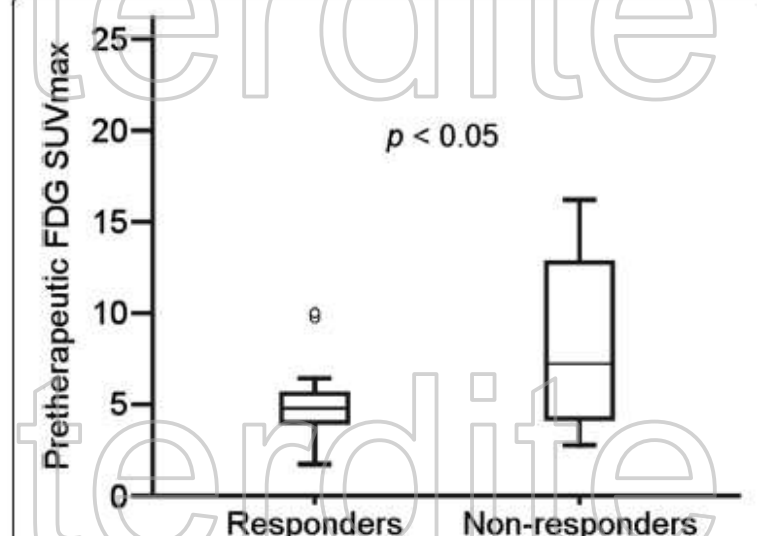


Figure 3 Comparison of pretherapeutic FDG SUVmax between responders and non-responders. The median value and the interquartile range are represented by box plot.

Copie Interdite

Table 2 Comparison of FDG accumulation and intratumoral distribution between responders and non-responders

Responder (n = 26)	Non-responder (n = 16)	p value
SUVmax	4.8 ± 2.0	8.5 ± 4.7
Skewness	1.07 ± 0.29	1.17 ± 0.40
Kurtosis	3.56 ± 0.91	3.99 ± 1.34
AUC-CSH	0.30 ± 0.05	0.30 ± 0.06

n. s., not significant.

Table 3 Comparison of ^{113}In -ibritumomab tiuxetan accumulation and intratumoral distribution between responders and non-responders

	Responder (n = 26)	Non-responder (n = 16)	p value
SUVmax	2.74 ± 1.43	3.29 ± 1.47	n. s.
% ID/g	0.0022 ± 0.0009	0.0024 ± 0.0008	n. s.
Skewness	0.58 ± 0.16	0.73 ± 0.24	<0.05
Kurtosis	2.39 ± 0.32	2.78 ± 0.53	<0.02
AUC-CSH	0.37 ± 0.04	0.34 ± 0.05	<0.05

n. s., not significant.

Indium-111–Labeled Trastuzumab Scintigraphy in Patients With Human Epidermal Growth Factor Receptor 2–Positive Metastatic Breast Cancer

Patrick J. Perik, Marjolijn N. Lab-De Hooge, Jourik A. Gietema, Winette T.A. van der Graaf, M. Alexander de Kort, Sharon Jonkman, Jos G.W. Kosterink, Dirk J. van Veldhuisen, Dirk T. Sleijfer, Pieter L. Jager, and Elisabeth G.E. de Vries

JCO 2006

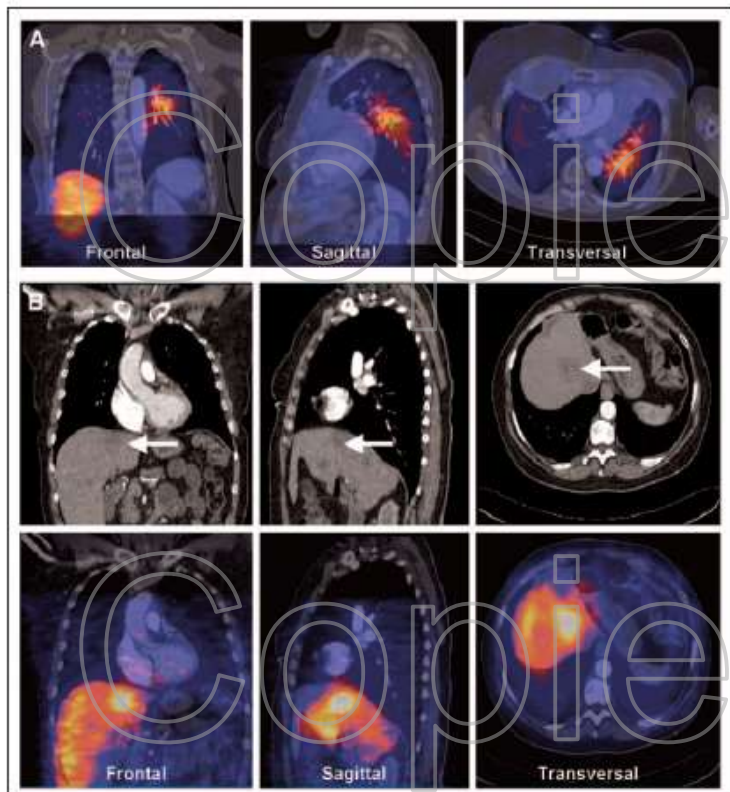


Fig 2. (A) Fused computed tomography (CT) with indium-111-diethylenetriamine penta-acetic acid anhydride (111In-DTPA)-trastuzumab single-photon emission tomography (SPECT) image 196 hours after tracer injection. (B) CT images (top) of a patient with a large liver metastasis (→). Fusion with 111In-DTPA-trastuzumab SPECT (bottom) shows correspondence of liver metastases and SPECT hot spot.

Associations between the uptake of ^{111}In -DTPA-trastuzumab, HER2 density and response to trastuzumab (Herceptin) in athymic mice bearing subcutaneous human tumour xenografts

EJNM 2009

Kristin McLarty • Bart Cornelissen •

Deborah A. Scollard • Susan J. Done • Kathy Chun •

Raymond M. Reilly

Conclusions

1. HER2 expression : Semi quantification : vers un SUV_{SPECT}?
2. Fixation non Spécifique : LE FOIE
3. Fixation tumorale de ^{111}In -DTPA-trastuzumab associée à T réponse

Evaluation of [¹⁸F]gefitinib as a molecular imaging probe for the assessment of the epidermal growth factor receptor status in malignant tumors

Helen Su · Yann Seimbille · Gregory Z. Ferl ·

Claudia Bodenstein · Barbara Fueger · Kevin J. Kim ·

Yu-Tien Hsu · Steven M. Dubinett · Michael E. Phelps ·

Johannes Czernin · Wolfgang A. Weber

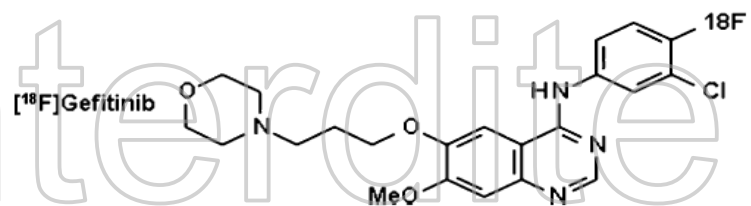
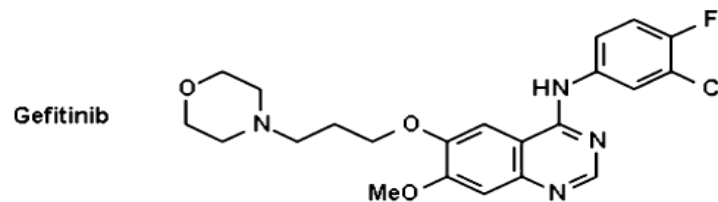


Fig. 1 Chemical structure of gefitinib and [¹⁸F]gefitinib

Conclusions

1.[¹⁸F]- gefitinib = PK.

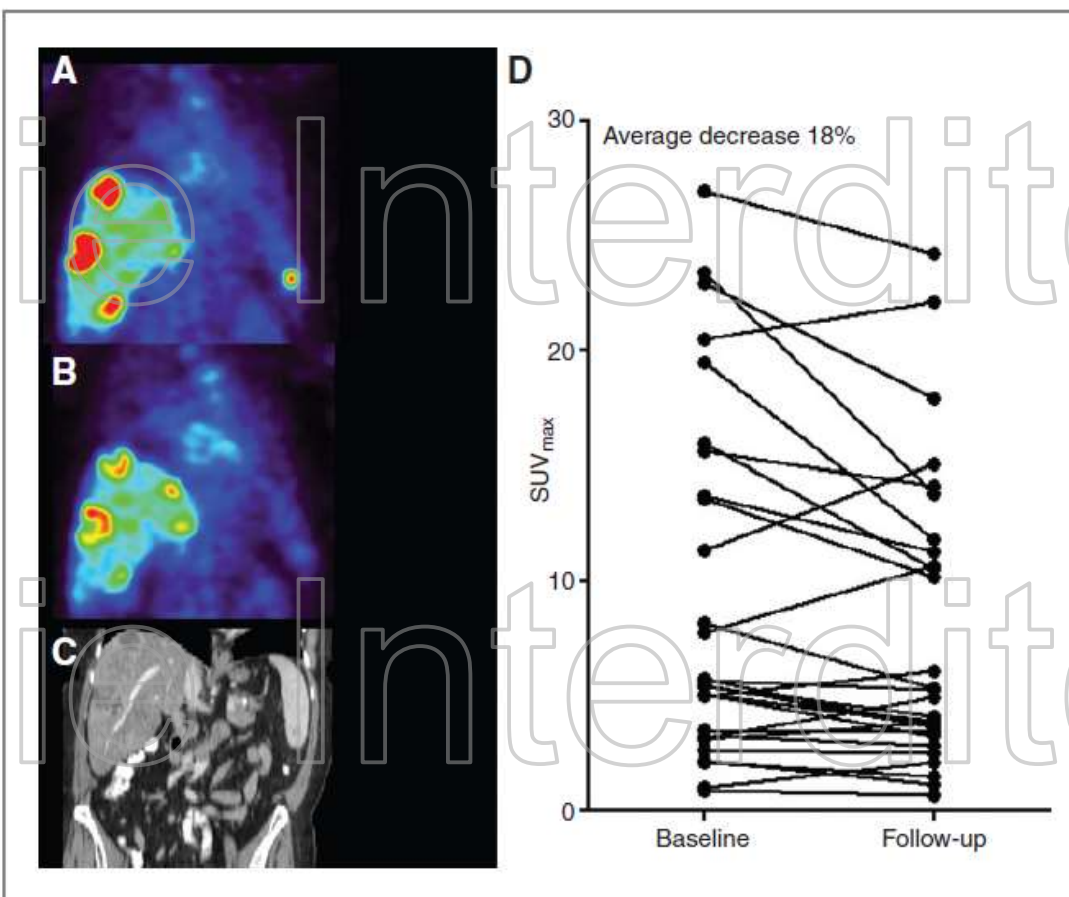
2.Pb, fixation non spécifique

⁸⁹Zr-trastuzumab and ⁸⁹Zr-bevacizumab PET to Evaluate the Effect of the HSP90 Inhibitor NVP-AUY922 in Metastatic Breast Cancer Patients

Sietske B.M. Gaykema¹, Carolien P. Schröder¹, Joanna Vitfell-Rasmussen⁵, Sue Chua⁵, Thijs H. Oude Munnink¹, Adrienne H. Brouwers², Alfons H.H. Bongaerts³, Mikhail Akimov^{6,7}, Cristina Fernandez-Ibarra^{6,7}, Marjolijn N. Lub-de Hooge^{2,4}, Elisabeth G.E. de Vries¹, Charles Swanton⁵, and Uday Banerji⁵

DEUX CIBLES
ErbB2,
VEGF

Figure 2. Representative coronal ⁸⁹Zr-trastuzumab PET images of a patient scanned before (A) and after (B) 3 weeks of treatment. Multiple liver lesions and one splenic lesion are shown. ⁸⁹Zr-trastuzumab PET could be performed in 6 of 10 HER2-positive patients, of which 5 underwent repeated scan procedures. The CT scan pretreatment is shown in C. D, a heterogeneous response in individual tumor lesions ($n = 29$) between baseline and follow-up, with an average decrease in SUV_{max} of 18%.



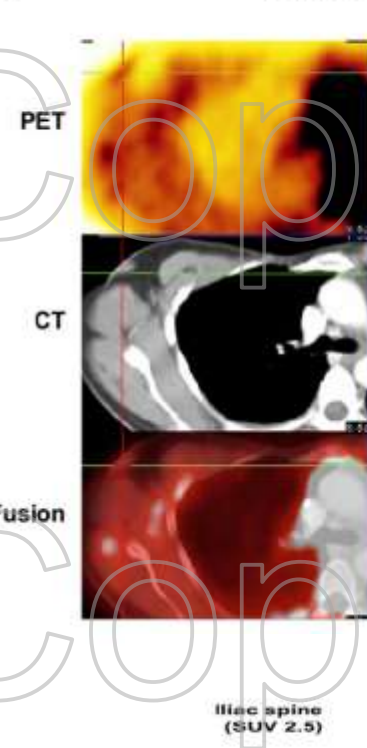
The smaller the better ?

On the Selection of a Tracer for PET Imaging of HER2-Expressing Tumors: Direct Comparison of a ^{124}I -Labeled Affibody Molecule and Trastuzumab in a Murine Xenograft Model

Anna Orlova^{1,2}, Helena Wallberg¹, Sharon Stone-Elander³, and Vladimir Tolmachev^{1,2,4}

Molecular Imaging of HER2-Expressing Malignant Tumors in Breast Cancer Patients Using Synthetic ^{111}In - or ^{68}Ga -Labeled Affibody Molecules

Richard P. Baum¹, Vikas Prasad¹, Dirk Müller¹, Christiane Schuchardt¹, Anna Orlova^{2,3}, Anders Wennborg²,
Vladimir Tolmachev^{2,3}, and Joachim Feldwisch^{2,3}

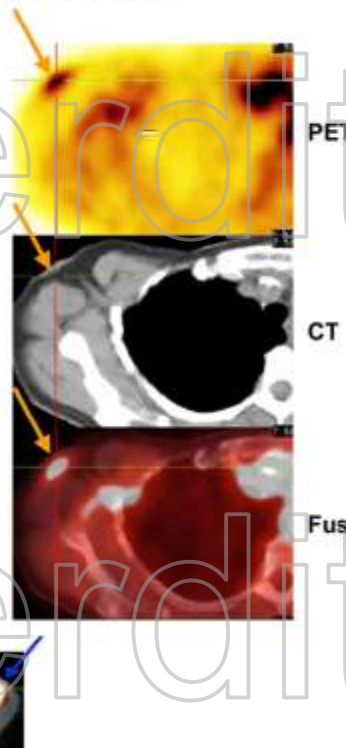
A**¹⁸F-FDG PET/CT**

Soft tissue of
the musculus
glutaeus
minimus
close to the
iliac bone
(SUV 4.3)

Femur head
(SUV 2.1)

Musculus
sartorius
(SUV 2.4)

Potential
lymphangiosis
within the
musculus
quadriceps
(SUV 2.6)

⁶⁸Ga-ABY-002 PET/CT

Yellow arrowheads point to the iliac spine in both the PET and Fusion images.

Green arrowheads point to the femur head in both the PET and Fusion images.

Blue arrowheads point to the muscle tissue in both the PET and Fusion images.

Red arrowheads point to the potential lymphangiosis in the quadriceps muscle in both the PET and Fusion images.

Copie Interdite

Perspectives

Copie Interdite

Quand l'imagerie sert à la pharmacocinétique !



ELSEVIER

Advanced Drug Delivery Reviews 63 (2011) 539–546

Contents lists available at ScienceDirect

Advanced Drug Delivery Reviews

journal homepage: www.elsevier.com/locate/addr



Approaches using molecular imaging technology – use of PET in clinical microdose studies[☆]

Claudia C. Wagner^a, Oliver Langer^{a,b,*}

^a Department of Clinical Pharmacology, Medical University of Vienna, Währinger-Gürtel 18-20, A-1090, Vienna, Austria

^b Health & Environment Department, Molecular Medicine, AIT Austrian Institute of Technology GmbH, A-2444 Seibersdorf, Austria



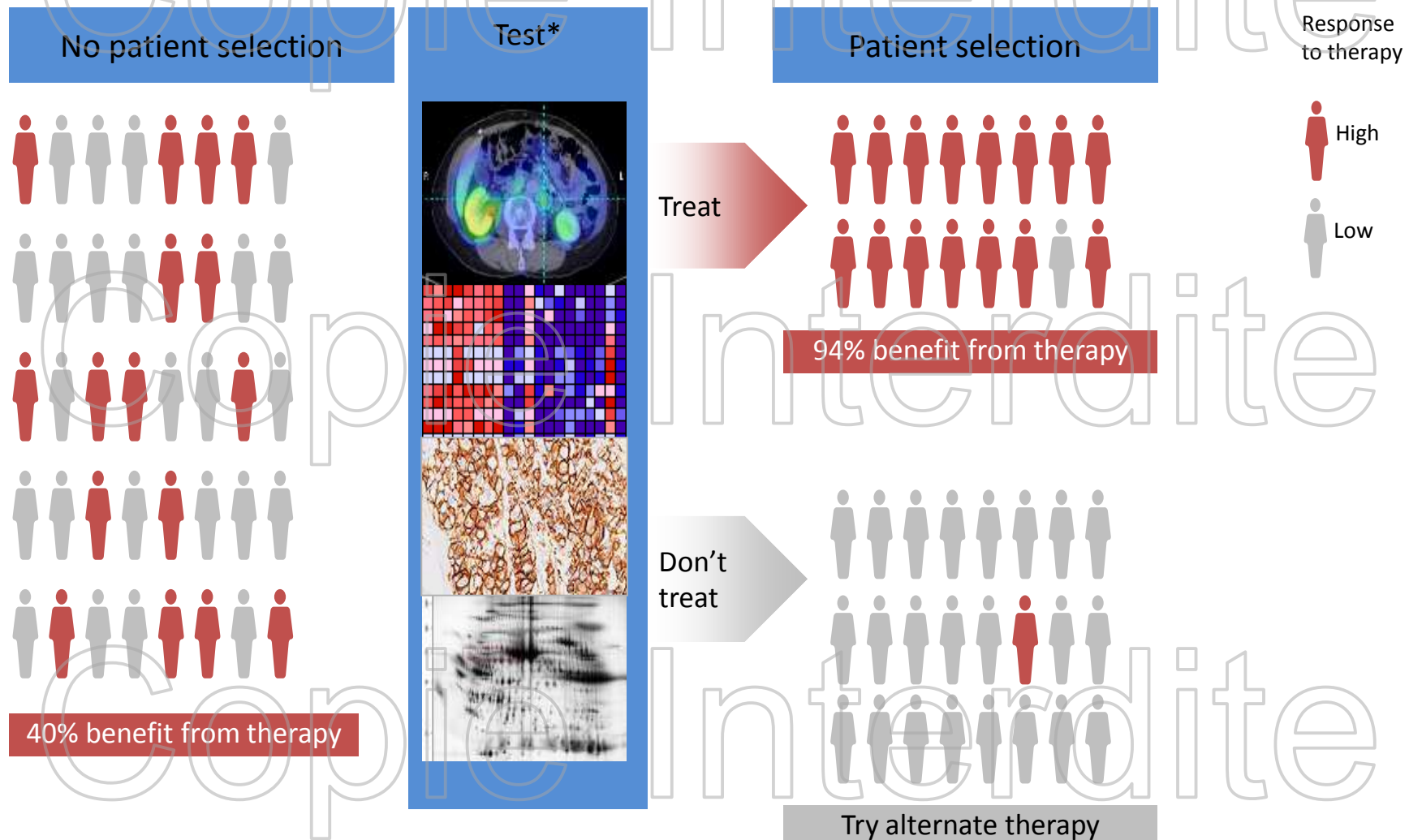
The European Agency for the Evaluation of Medicinal Products
Evaluation of Medicines for Human Use

London, 23 January 2003
CPMP/SWP/2599/02

COMMITTEE FOR PROPRIETARY MEDICINAL PRODUCTS
(CPMP)

POSITION PAPER ON NON-CLINICAL SAFETY STUDIES TO
SUPPORT CLINICAL TRIALS WITH A SINGLE MICRODOSE

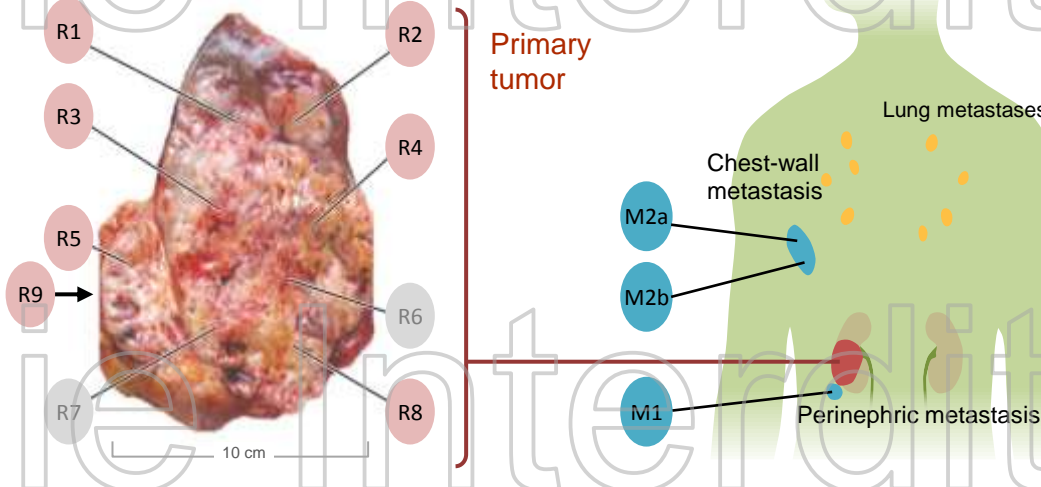
DATA MINING



* Blood, tissue or imaging marker that can be used to prospectively identify patients

Pénétrer dans la cible

Intra and inter-tumor heterogeneity



The NEW ENGLAND
JOURNAL of MEDICINE

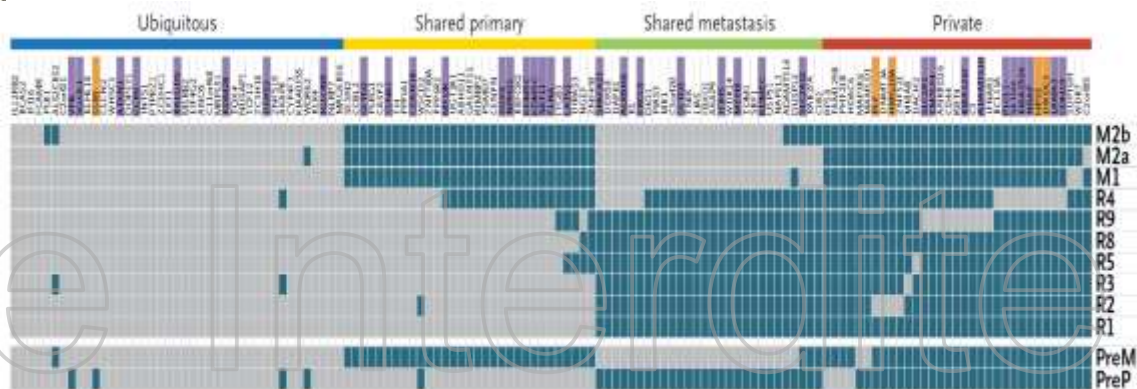
ESTABLISHED IN 1812

MARCH 8, 2012

VOL. 366 NO. 10

Intratumor Heterogeneity and Branched Evolution Revealed
by Multiregion Sequencing

Gerlinger et al. N Engl J Med 2012



Cetuximab Shows Activity in Colorectal Cancer Patients With Tumors That Do Not Express the Epidermal Growth Factor Receptor by Immunohistochemistry

Ki Young Chung, Jinru Shia, Nancy E. Kemeny, Manish Shah, Gary K. Schwartz, Archie Tse, Audrey Hamilton, Dorothy Pan, Deborah Schrag, Lawrence Schwartz, David S. Klimstra, Daniel Fridman, David P. Kelsen, and Leonard B. Saltz

JCO 2005

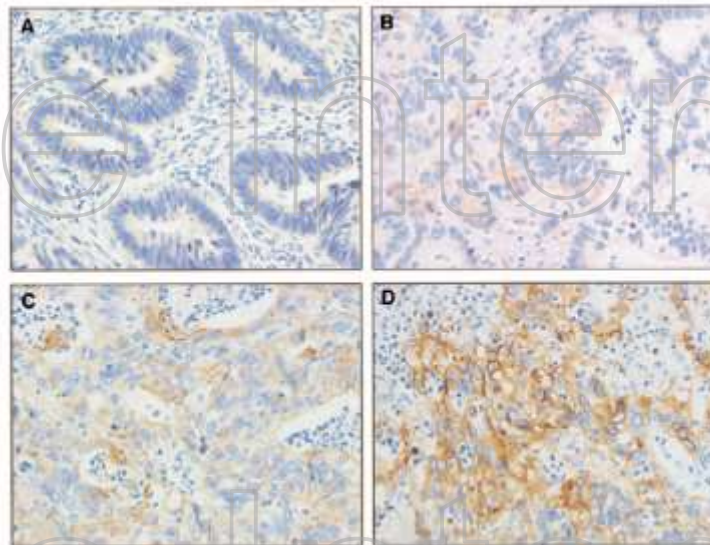
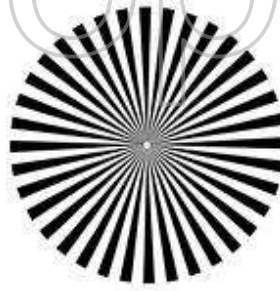
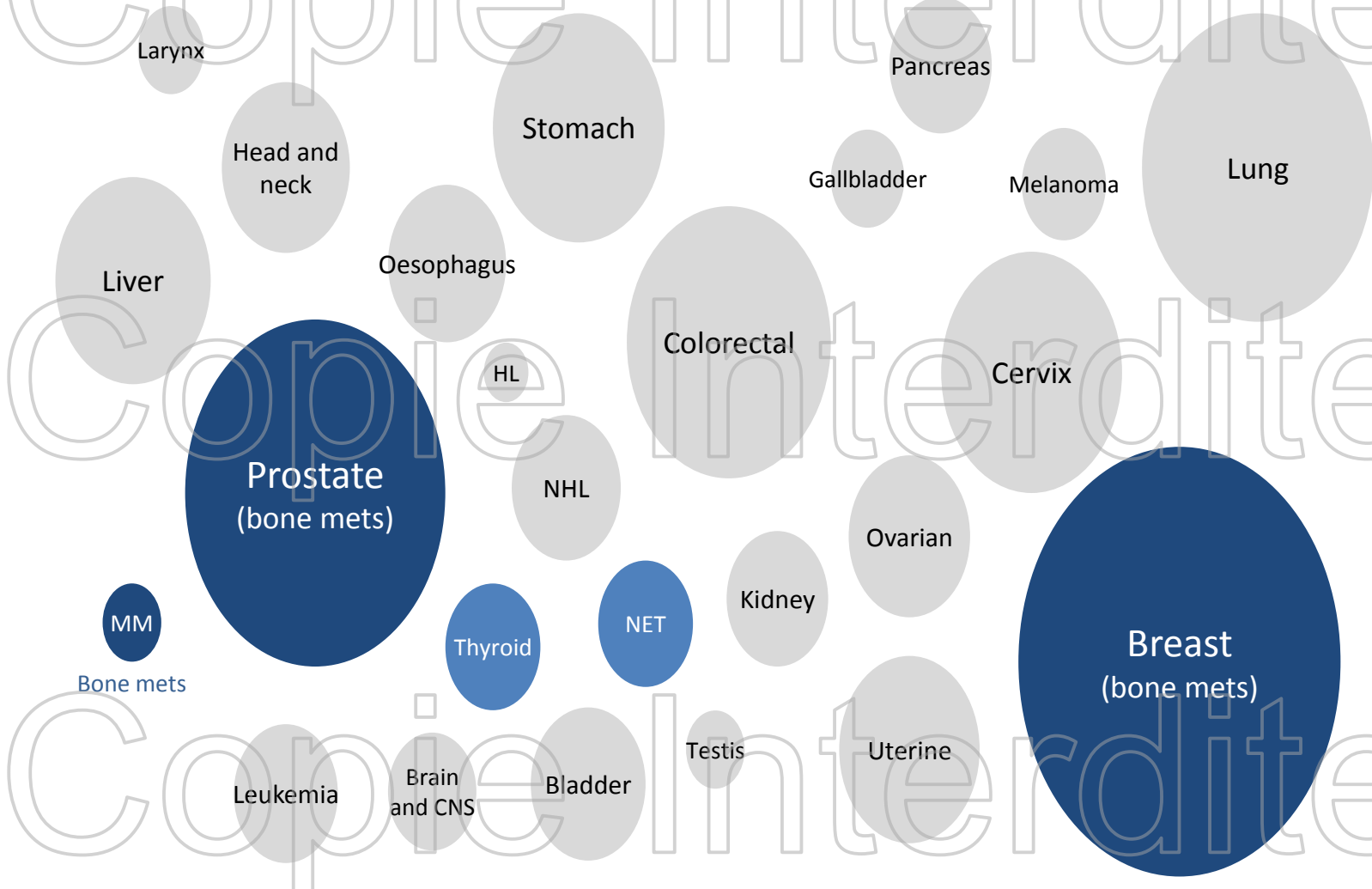


Fig 1 Representative epidermal growth factor receptor (EGFR) immunohistochemistry scoring. Level of EGFR staining: (A) 0; (B) 1+; (C) 2+; (D) 3+.

Imaging and the cancer landscape in the 1990s

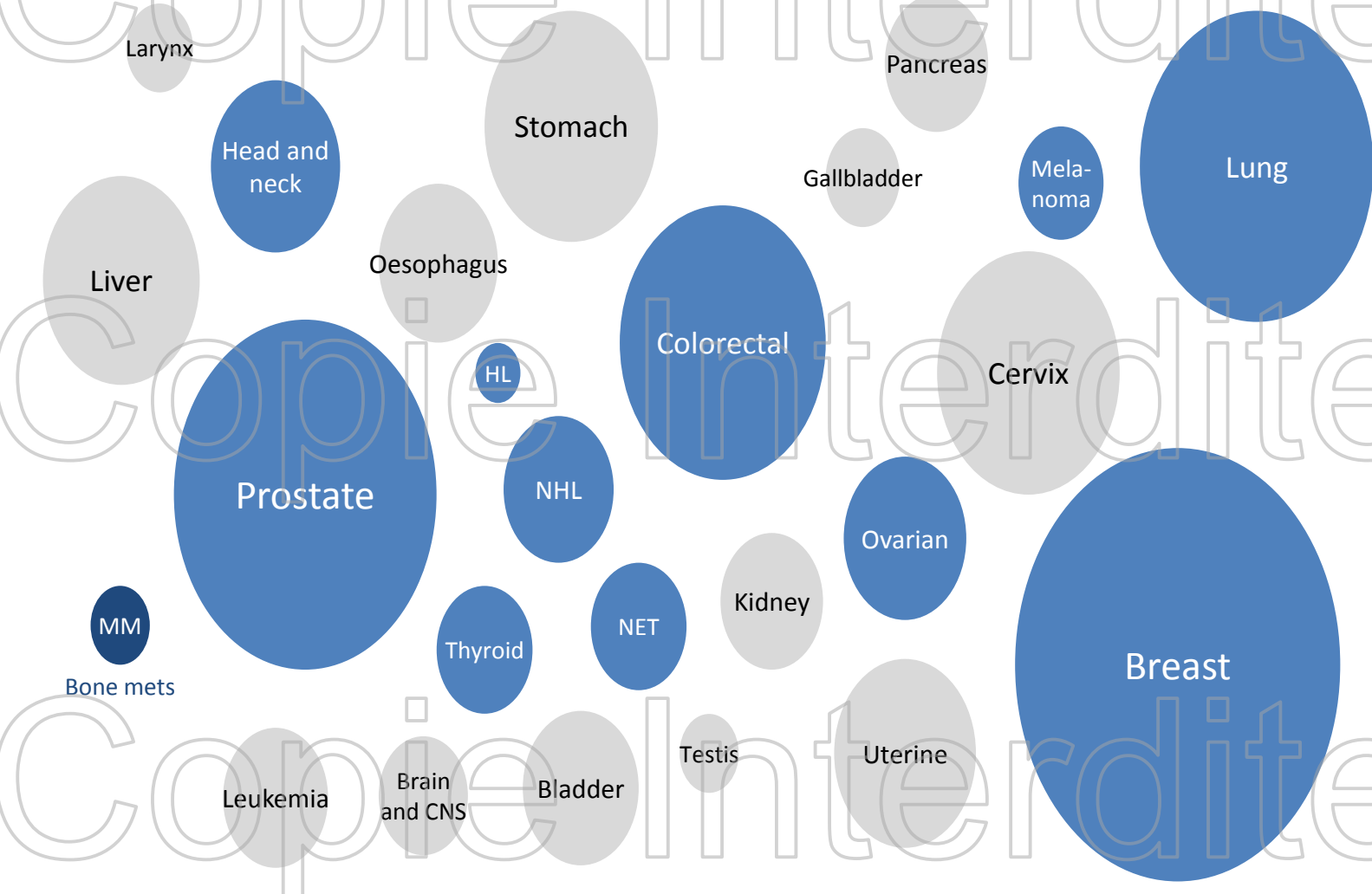


Structural imaging

Functional imaging

Size of bubble proportional to incidence, Globocan 2012
<http://globocan.iarc.fr>, estimated cancer incidence world

Imaging and the cancer landscape is changing rapidly



Structural imaging

Functional imaging

Size of bubble proportional to incidence, Globocan 2012
<http://globocan.iarc.fr>, estimated cancer incidence world

QUELLE APPROCHE THERANOSTIQUE POUR LE RADIUM . MDP. F Na, F CHOLINE

^{99m}Tc-MDP



Samarium/ strontium/ radium

diphosphonates

Médecine Nucléaire - Imagerie fonctionnelle et métabolique - 2006 - vol.30 - n°3



Dans le doute

Recent bisphosphonate therapy may reduce ⁸⁹Sr, ¹⁵³Sm-lexidronam or ¹⁸⁶Re-etidronate uptake by bone metastases and reduce the effectiveness of pain palliation. An interval of at least 48 h is recommended between bisphosphonate administration and ⁸⁹Sr, ¹⁵³Sm-lexidronam or ¹⁸⁶Re-etidronate treatment.

EJNM guidelines 2002

4.5 Interactions avec d'autres médicaments et autres formes d'interactions

Aucune étude clinique d'interaction n'a été réalisée.

Des interactions avec le calcium et le phosphate ne pouvant être exclues, il doit être envisagé de suspendre une supplémentation à base de ces traitements et/ou la prise de Vitamine D quelques jours avant le début du traitement par Xofigo.

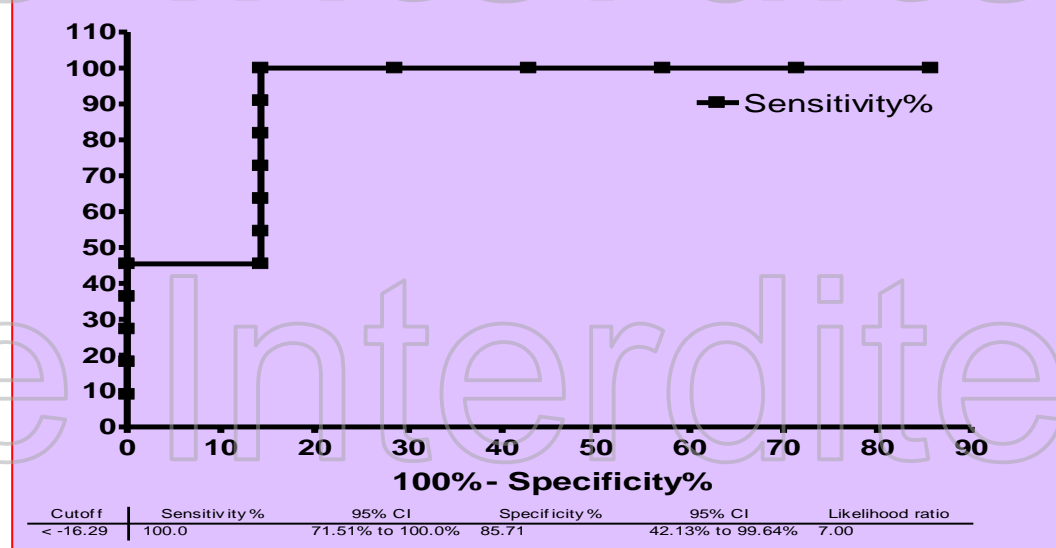
L'administration concomitante d'une chimiothérapie et de Xofigo peut produire des effets additifs en ce qui concerne la myélosuppression (voir rubrique 4.4). La sécurité d'emploi et l'efficacité de l'administration concomitante d'une chimiothérapie et de Xofigo n'ont pas été établies.

Xofigo® RCP

MR
Molecular response
nMR
No molecular
response

FDG vs pERK

(F Thomas Clin Can Res
2007, Delord et al –
Courbon et al Abs 2005-
2006)
SNM 2009
Soumis A Clin Cancer Res
2ème rev



Evolution de l'imagerie

structure

Bilan d'extension



Fonction

Diagnostic bilan d'extension

- Enriched tumor localisation
- Cancer metabolism
- Tumor staging

Intervention optimisée

- Track treatment response
- PERCIST
- Guides radiotherapy
- Guides surgery

Nomogramme thérapeutique/ taxonomie

- Patient matching
- Disease matching

Imagerie de phénotype

Métabolisme

- Glucose
- Choline
- Acetate

Expression de cible

- Tyrosine analogues
- VEGF
- RET/RTK
- Folate receptor

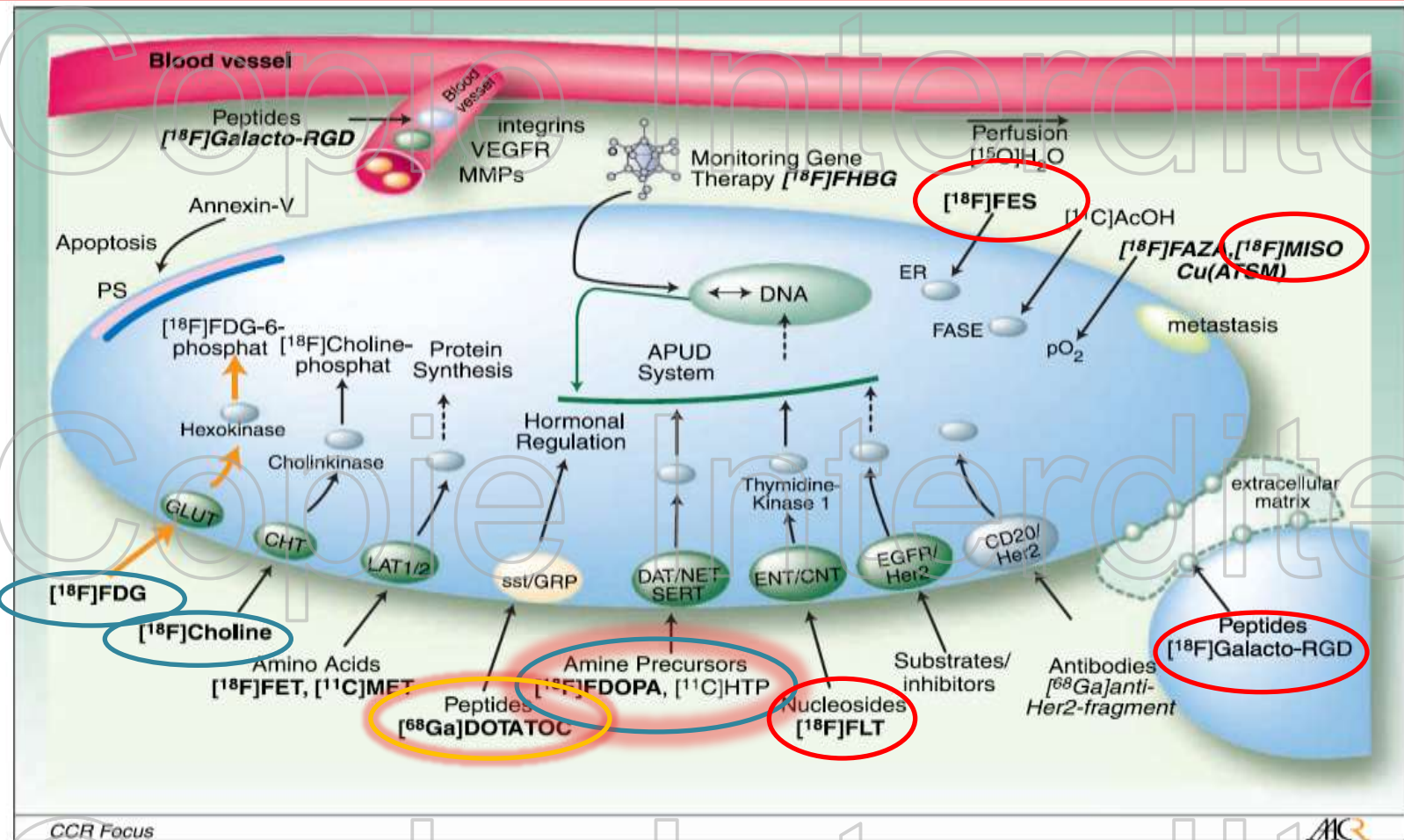


Fig. 2. Selected targets and corresponding nuclear imaging probes already established for nuclear molecular imaging in the clinic (**bold**) or currently under assessment in clinical studies (*italic*).

Copie Interdite

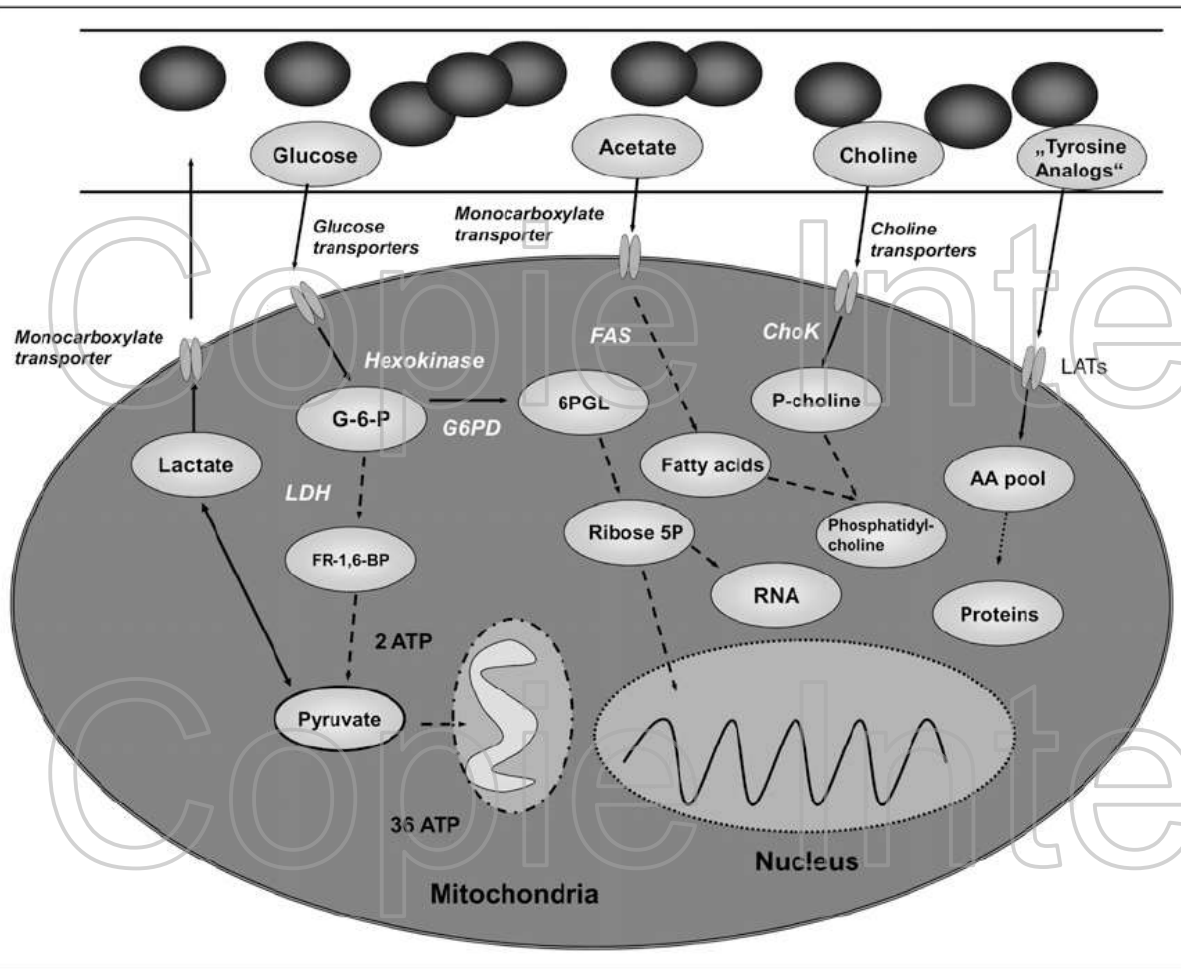


FIGURE 1. Simplified overview of metabolic processes targeted by PET and MRI. AA pool = amino acid pool; ChoK = choline kinase; FAS = fatty acid synthase; FR-1,6-BP = fructose-1,6-bisphosphate; G-6-P = glucose-6-phosphate; LAT = L-type amino acid transporter; LDH = lactate dehydrogenase; P-choline = phosphocholine; Ribose 5P = ribose-5-phosphate.